Electronic Supplementary Material (ESI) for Physical Chemistry Chemical Physics.

Supporting Information for "Novel two-dimensional silicon-carbon binaries by crystal structure prediction"

Pedro Borlido and Silvana Botti

Institut für Festkörpertheorie und -optik, Friedrich-Schiller-Universität Jena and European Theoretical Spectroscopy Facility, Max-Wien-Platz 1, 07743 Jena, Germany

Ahmad W. Huran and Miguel A. L. Marques

Institut für Physik, Martin-Luther-Universität Halle-Wittenberg, D-06099 Halle, Germany

I. General comments

Here we show the two-dimensional Brillouin zone of the orthorhombic structures, to clarify the choice of the paths for electronic and phonon band structures [1]. This Brillouin zone corresponds to the 2D section of the 3D cell required for calculations.

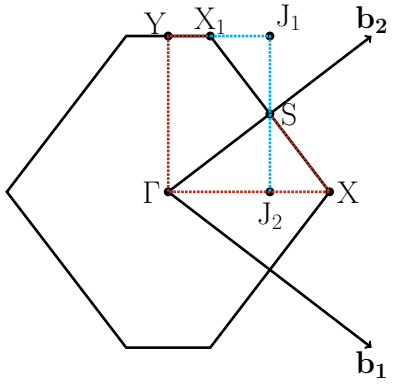

FIG. S-1. Two-dimensional Brillouin zone corresponding to the base-centered orthorhombic cell with real-space lattice vectors $a_1 = (a/2, b/2)$ and $a_2 = (a/2, -b/2)$. The coordinates of the indicated symmetry points are given explicitly in Table S-I.

TABLE S-I. Fractional coordinates in reciprocal lattice units of the symmetry points indicated in Figure S-1. Here $\eta = (1 + a^2/b^2)/4$, where a and b are the lattice constants of the conventional cell.

	$\mathbf{b_1}$	$\mathbf{b_2}$	$\mathbf{b_3}$
Γ	0	0	0
X	η	η	0
S	0	1/2	0
X_1	-η	1-η	0
Y	-1/2	1/2	0
J_1	-1/4	3/4	0
J_2	1/4	1/4	0

II. Carbon-rich crystal structures

Here we present more information related to the carbon-rich ($x < 0.5$) structures discussed in the main text.

In Figure S-2 we show the lowest-energy polymorphs found by the minima-hopping method at different $x < 0.5$ stoichometries. SiC_4-SI and SiC_5-SI are ordered alloys of graphene polymorphs. SiC_3-SI and SiC_6-SI can be viewed as graphene nanoribbons connected via silicon atoms. This type of construction, that can be found along the carbon-rich part of the phase diagram, generally creates bridges (e.g. SiC_6-SI) or steps (e.g. SiC_3-SI) of different sizes.

In Figure S-4 we present the charge density profiles of the bands close to the Fermi energy for SiC_2-b. For the last occupied band, we can see a curious sinusoidal pattern.

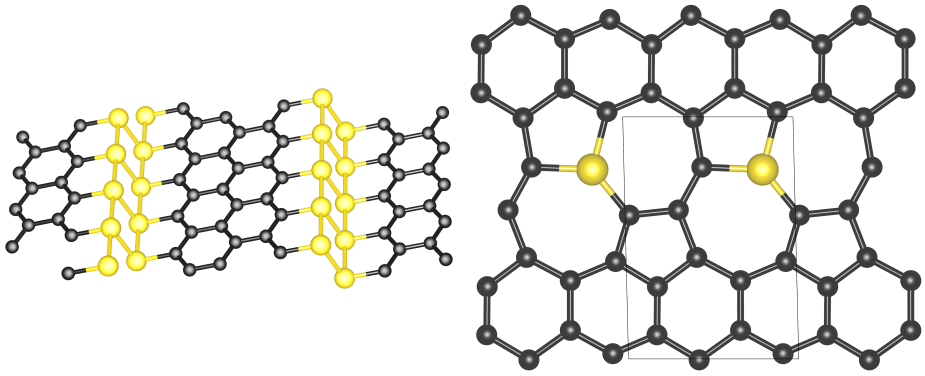

(a) SiC_3-SI (b) SiC_4-SI

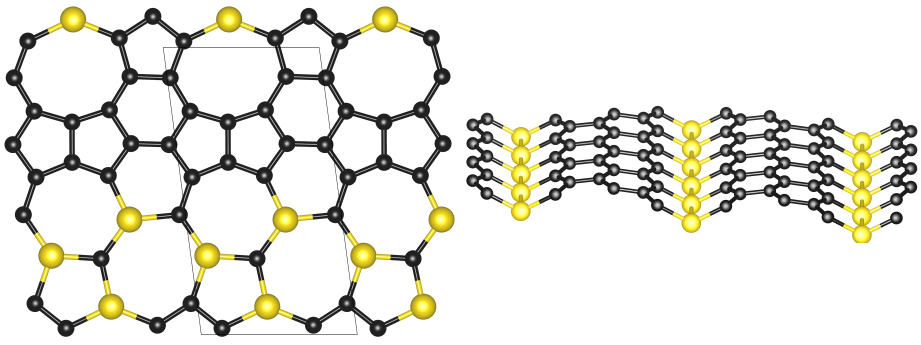

(c) SiC_5-SI (d) SiC_6-SI

FIG. S-2. Crystal structures of the lowest-energy polymorphs found by the minima-hopping method at the indicated stoichometries.

TABLE S-II. Coordinates of the atoms in SiC_6-SW. Conventional cell parameters are $a = 5.32$ Å and $b = 8.10$ Å. The x and y coordinates are given in fractional coordinates of the lattice vectors ($\mathbf{a} = (a/2, b/2, 0)$ and $\mathbf{b} = (a/2, -b/2, 0)$). The z coordinate is given in Å.

Atom	x	y	z (Å)
Si(1)	0.500	0.500	0.213
C(1)	0.070	0.400	0.426
C(2)	0.930	0.600	0.426
C(3)	0.400	0.070	0.000
C(4)	0.088	0.912	0.213
C(5)	0.912	0.088	0.213
C(6)	0.600	0.930	0.000

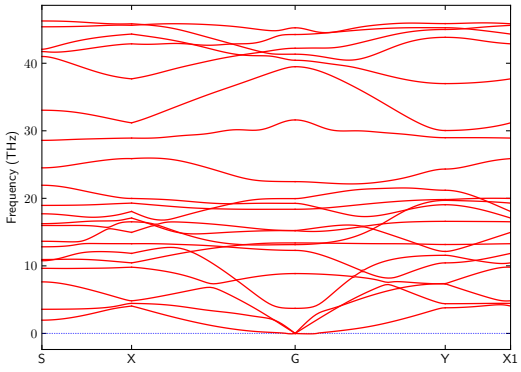

FIG. S-3. Phonon band structures obtained with DFTB for the SiC_6-SW polymorph. This figure was obtained with the finite difference method (as implemented in PHONOPY) using a $32 \times 32 \times 8$ k-point grid and a $9 \times 9 \times 1$ supercell. Due to being metallic and the soft nature of the out-of-plane modes, convergence for this structure was found to be particularly difficult, especially using DFT.

TABLE S-III. Coordinates of the atoms in SiC_2-b. Conventional cell parameters $a = 5.52$ Å and $b = 7.20$ Å. The x and y coordinates are given in fractional coordinates of the lattice vectors ($\mathbf{a} = (a/2, b/2, 0)$ and $\mathbf{b} = (a/2, -b/2, 0)$). The z coordinate is given in Å.

Atom	x	y	z (Å)
Si(1)	0.250	0.750	0.672
Si(2)	0.750	0.250	0.672
C(1)	0.844	0.656	1.344
C(2)	0.344	0.156	0.000
C(3)	0.156	0.344	0.000
C(4)	0.656	0.844	1.344

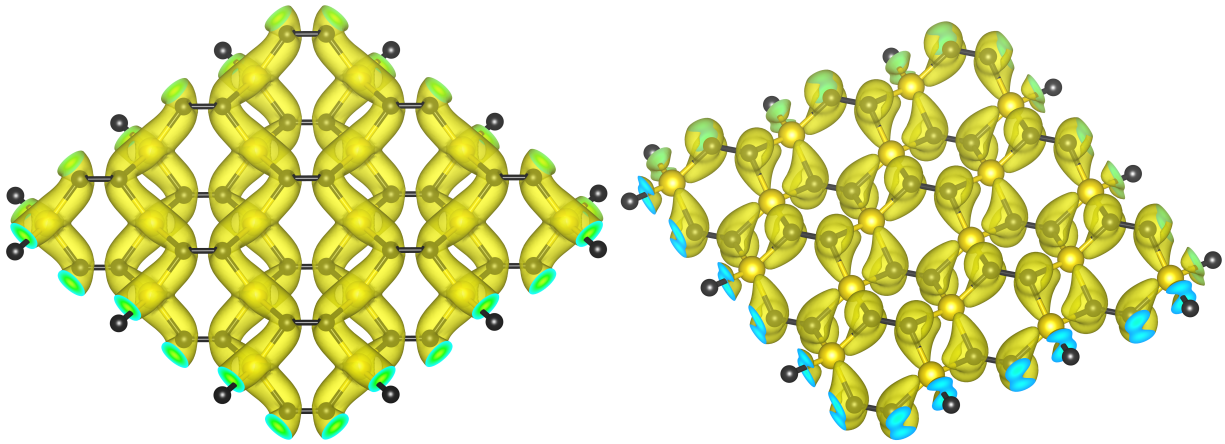

FIG. S-4. Charge density profiles of SiC_2-b for the band directly below (left) and above (right) the Fermi level.

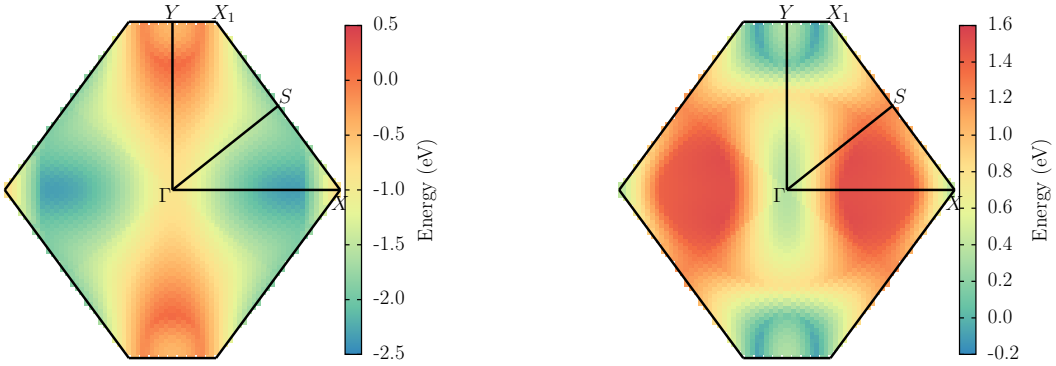

FIG. S-5. Heatmap of the two bands crossing the Fermi level of SiC_2-b: bottom (left) and top (right). Note the two different energy scales on the two images. Here the nature of the band interception at Y is visible. One can also see the reason behind the cone structure around X, caused by the shape of the Brillouin zone and the chosen path.

III. Bilayers

As mentioned in the main text, several low-energy structures at $x = 0.5$ are bilayers of 2D SiC. Some of them correspond to hexagonal stackings of alloyed monolayers (e.g. SiC-SI depicted in Fig. S-6 and SiC-SII depicted in Fig. S-7) and were already studied in the literature. We nonetheless present them here for the sake of completeness. SiC-SIII (Fig. S-8) is formed by two different types of SiC monolayers of the honeycomb family. It is a semiconductor with a gap of 0.63 eV, considerably lower than the other bilayers under study.

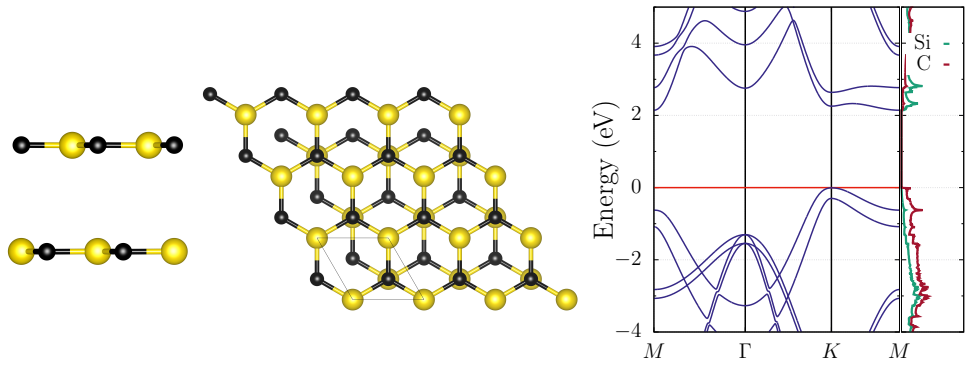

(a) (b) (c)

FIG. S-6. Lateral profile (a), top view (b) and electronic band structure (c) of the SiC-SI bilayer. This structure lies 0.29 eV above the convex hull.

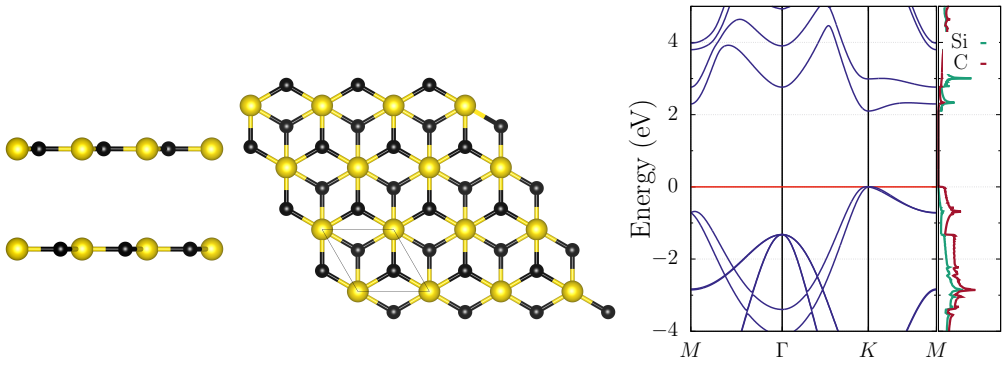

(a) (b) (c)

FIG. S-7. Lateral profile (a), top view (b) and electronic band structure (c) for the SiC-SII bilayer. This structure lies 0.30 eV above the convex hull.

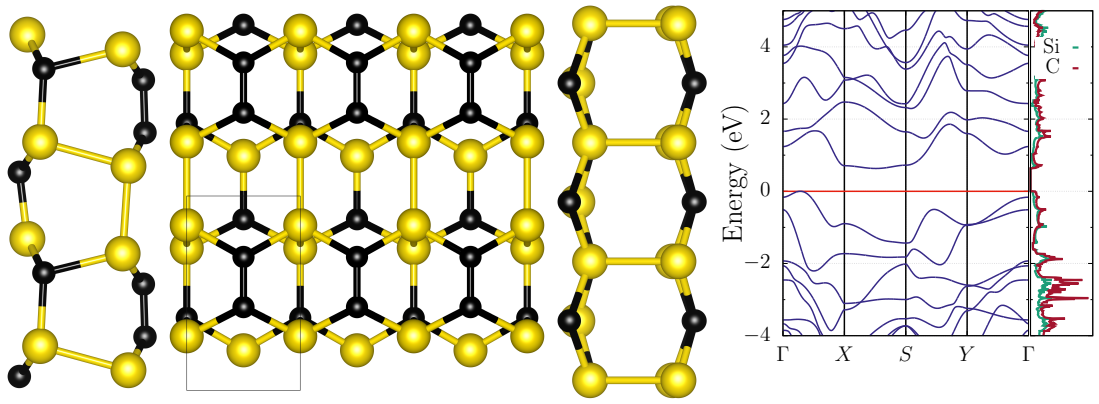

(a) (b) (c) (d)

FIG. S-8. Crystal structure of SiC-SIII viewed from the [100] direction (a) [001] direction (b) [010] direction (c). This structure lies 0.43 eV above the convex hull.

TABLE S-IV. Coordinates of the atoms in SiC-bi. The lattice parameter is $a = 3.16$ Å. The x and y coordinates are given in fractional coordinates of the lattice vectors ($\mathbf{a} = (a, 0)$ and $\mathbf{b} = (-a/2, a\sqrt{3}/2)$). The z coordinate is given in Å.

Atom	x	y	z (Å)
Si(1)	0.333	0.667	0.155
Si(2)	0.667	0.333	2.173
C(1)	0.333	0.667	2.323
C(2)	0.667	0.333	0.000

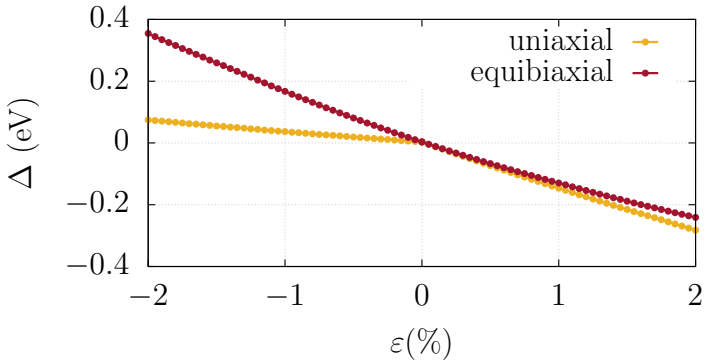

FIG. S-9. Variation of the band gap ($\Delta = E^{\text{gap}}(\varepsilon) - E^{\text{gap}}(\varepsilon = 0)$) of SiC-bi (calculated at fixed cell) for equibiaxial and uniaxial strain along the zigzag direction.

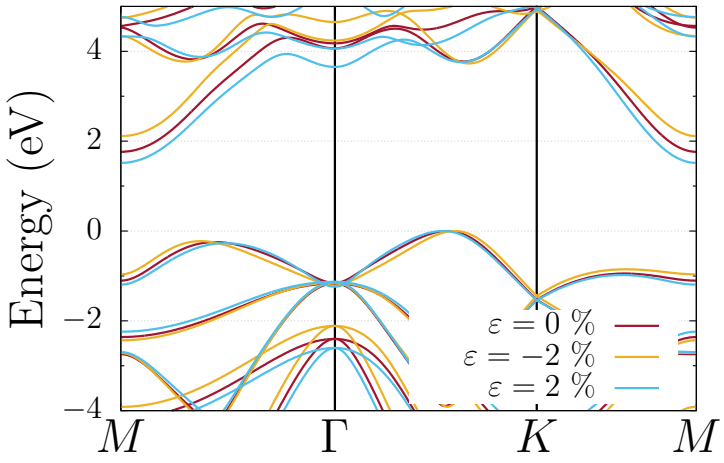

FIG. S-10. Electronic band structure for the SiC-bi structure obtained for different values of equibiaxial strain ($\varepsilon_{xx} = \varepsilon_{yy} = \varepsilon$). As seen from this figure, the qualitative nature of the band gap does not change within the tested range of strain.

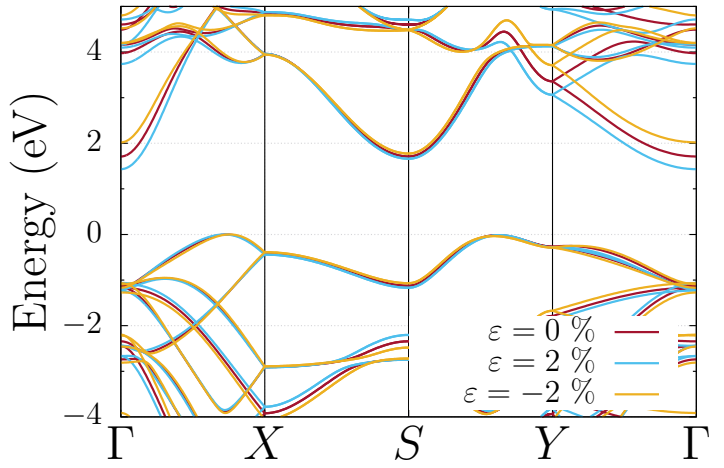

FIG. S-11. Electronic band structure for the SiC-bi structure obtained for different values of uniaxial strain along the zigzag direction ($\varepsilon_{xx} = \varepsilon$, $\varepsilon_{yy} = 0$). The band structure was computed using the rectangular supercell. As seen from this figure, there is a qualitative change in the conduction minima between positive and negative strain. This explains the change of slope seen in Figure S-9.

IV. Silicon-rich structures

We present here some information regarding the silicon-rich part of the phase diagram. In Figure S-12 we show the structures stemming from the exhaustive enumeration that lie between the two convex-hulls shown in Fig. 1 of the main article. The naming convention reflects the position with respect to the lowest energy structure at the given composition (e.g. Si_nC_m-II would be the second lowest energy structure at the n:m ratio).

TABLE S-V. Coordinates of atoms in Si_3C-I. Conventional cell parameters are $a = 3.05$ Å and $b = 5.97$ Å. The x and y coordinates are given in fractional coordinates of the lattice vectors ($\mathbf{a} = (a, 0)$ and $\mathbf{b} = (0, b)$). The z coordinate is given in Å.

Atom	x	y	z (Å)
Si(1)	0.000	0.857	1.853
Si(2)	0.000	0.820	5.103
Si(3)	0.500	0.575	3.839
Si(4)	0.500	0.192	3.452
Si(5)	0.500	0.368	1.340
Si(6)	0.000	0.140	0.000
C(1)	0.500	0.670	2.323
C(2)	0.000	0.015	3.558

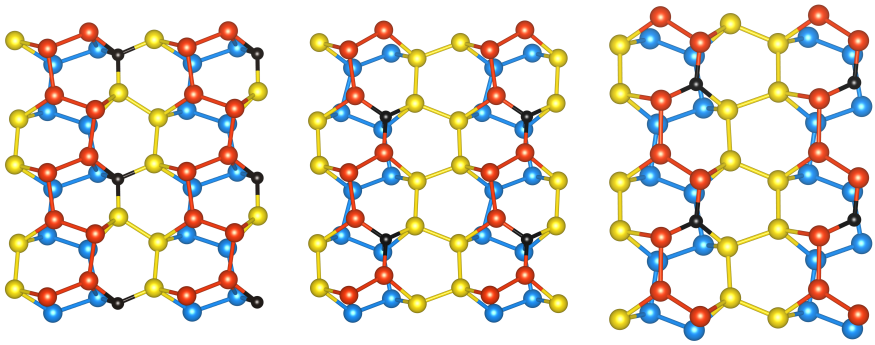

(a) $Si_{11}C_1$-I (b) $Si_{11}C_1$-II (c) $Si_{11}C_1$-III

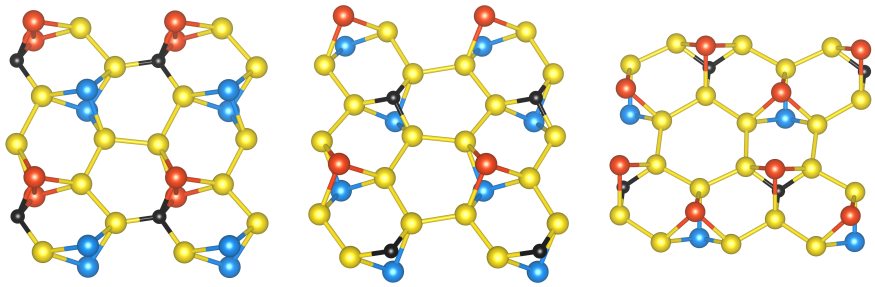

(d) Si_9C_1-I (e) Si_9C_1-II (f) Si_9C_1-IV

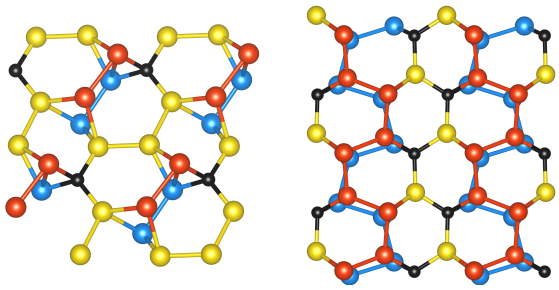

(g) Si_7C_1-I (h) Si_5C_1-I

FIG. S-12. Crystal structures of some of the polymorphs present in Fig. 1 of the main article. Each structure is labelled according to its chemical composition and its relative energy ordering (indicated by the corresponding Roman numeral). Carbon atoms are presented in black (regardless of their position) while silicon atoms are coloured blue, yellow or red depending if they are below, in or above the middle plane, respectively.

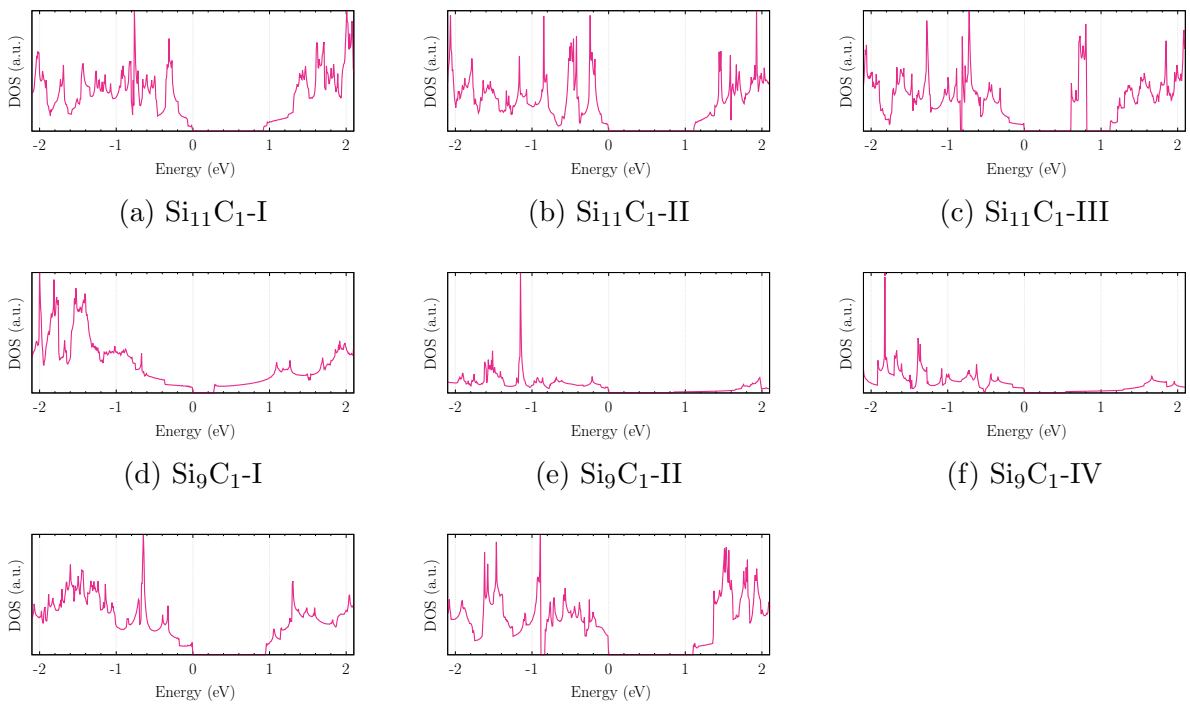

(a) $Si_{11}C_1$-I (b) $Si_{11}C_1$-II (c) $Si_{11}C_1$-III

(d) Si_9C_1-I (e) Si_9C_1-II (f) Si_9C_1-IV

(g) Si_7C_1-I (h) Si_5C_1-I

FIG. S-13. (Spin-up) Total densities of state the polymorphs present in Fig. S-12.

TABLE S-VI. Coordinates of atoms in Si_3C-II. Conventional cell parameters are $a = 2.99$ Å and $b = 5.96$ Å. The x and y coordinates are given in fractional coordinates of the lattice vectors ($\mathbf{a} = (a, 0)$ and $\mathbf{b} = (0, b)$). The z coordinate is given in Å.

Atom	x	y	z (Å)
Si(1)	0.250	0.957	3.643
Si(2)	0.750	0.043	1.547
Si(3)	0.250	0.648	5.189
Si(4)	0.750	0.352	0.000
Si(5)	0.250	0.554	1.594
Si(6)	0.750	0.445	3.595
C(1)	0.250	0.862	1.734
C(2)	0.750	0.138	3.455

[1] Wahyu Setyawan and Stefano Curtarolo. High-throughput electronic band structure calculations: Challenges and tools. *Comput. Mater. Sci.*, 49(2):299–312, August 2010. ISSN 09270256. doi:10.1016/j.commatsci.2010.05.010.